

C.S. Chern
C.W. Liu

Effect of short-chain alcohols on the oil-in-water microemulsion polymerization of styrene

Received: 24 August 1999

Accepted in revised form: 22 October 1999

C.S. Chern (✉) · C.W. Liu
Department of Chemical Engineering
National Taiwan University of Science
and Technology
43 Keelung Road, Section 4
Taipei 106, Taiwan
Fax: +886-2-27376644
e-mail: chern@ch.ntust.edu.tw

Abstract The influence of short-chain alcohols, 1-butanol (C_4OH), 2-pentanol (C_5OH) and 1-hexanol (C_6OH), on the formation of oil-in-water styrene microemulsions and the subsequent free-radical polymerization was studied. Sodium dodecyl sulfate was used as the surfactant. The overall performance of C_4OH as the cosurfactant is quite different from C_5OH and C_6OH . The range of the microemulsion region in decreasing order is $C_4OH > C_5OH > C_6OH$. The primary parameters selected for the microemulsion polymerization study were the concentrations of cosur-

factant and styrene. Only a small fraction of microemulsion droplets initially present in the reaction system can be successfully transformed into latex particles and the remaining droplets serve as a reservoir to supply the growing particles with monomer. Limited flocculation of latex particles also occurs during polymerization and the degree of flocculation is most significant for the C_4OH system.

Key words Oil-in-water microemulsion polymerization · Styrene · Sodium dodecyl sulfate · Short-chain alcohols

Introduction

Oil-in-water (O/W) microemulsions consist of oil droplets (1–10 nm in diameter) dispersed in water with the aid of surfactant (e.g., sodium dodecyl sulfate, SDS) and cosurfactant (e.g., 1-pentanol, C_5OH) [1]. Schulman and coworkers [2–4] contributed significantly to the pioneering work on microemulsions. Incorporation of amphipathic C_5OH into the adsorbed layer of SDS around the droplet greatly reduces the electrostatic repulsion force between two SDS molecules, minimizes the oil–water interfacial tension and decreases the persistence length of the interfacial layer (i.e., enhances the flexibility of the interfacial membrane). All these synergistic factors promote the spontaneous formation of transparent one-phase microemulsions exhibiting excellent fluidity. Unlike macroemulsions and miniemulsions, homogenization is not required in the formation of microemulsions and the colloidal product is thermodynamically stable. If a vinyl mono-

mer such as styrene (ST) is used as the component of the dispersed phase, stable nanoparticles (10 nm) comprising only a few polystyrene chains with high molecular weight can be produced via free-radical polymerization (termed microemulsion polymerization) [5–13]. Microemulsion polymerization mechanisms and kinetics were the subjects of these studies. Nevertheless, the systematic study of the influence of short-chain alcohols [1-butanol (C_4OH), (C_5OH) and 1-hexanol (C_6OH)] on the formation of ST microemulsions and subsequent polymerization inside the extremely small monomer droplets has been scarce. The objective of this work was therefore to establish the pseudo three-component phase diagram for the SDS/ C_iOH ($i = 4–6$) -stabilized ST microemulsions by the naked eye in combination with viscosity [14] and conductivity [15–17] measurements. Another major objective of this project was to study the effect of C_iOH on the ST microemulsion polymerization using a water-soluble persulfate initiator.

Experimental

Materials

The materials used were ST (Taiwan Styrene Co.), SDS (J. T. Baker), methanol (Acros), C_4OH (Acros), C_5OH (Janssen Chimica), C_6OH (Riedel-de Haen), $Na_2S_2O_8$ (Riedel-de Haen), $NaHCO_3$ (a buffer reagent) (Janssen Chimica), tris(hydroxymethyl)amino-methane (Acros), nitrogen (Ching-Feng-Harng Co.) and deionized water (Barnsted Nanopure Ultrapure Water System, specific conductance $<0.057 \mu S/cm$). The monomer was distilled under reduced pressure before use. All other chemicals were used as received.

Preparation of microemulsion

As an example, C_5OH (about 0.1 g each time) was added successively to the milky macroemulsion comprising 25 g water, 2.75 g SDS and 1.48 g ST with mild mixing at room temperature. The transitions from the milky macroemulsion to the transparent microemulsion and then to the lamellar gel phase were observed visually. By changing the amount of ST (0.5–3.5 g) in the initial macroemulsion and repeating the C_5OH titration procedure, the pseudo three-component phase diagram was constructed. Note that the microemulsion region identified in this way is by no means accurate and it needs verification by independent measurements of viscosity (Brookfield LVT) and conductivity (Orion 115).

Microemulsion polymerization

A typical recipe consists of 25 g water, 2.75 g (381 mM) SDS, 1 g (453 mM) C_5OH , 1.48 g ST, 0.5 mM $Na_2S_2O_8$ and 0.1 mM $NaHCO_3$, in which the molar concentration is based on total water. Before the start of polymerization, the reaction medium was purged with nitrogen for 20 min. Batch microemulsion polymerization was carried out in a 100-ml reactor at 70 °C for 8 h. The latex product was filtered through a 200-mesh (0.074-mm) screen to collect the filterable solids. The latex particle size (d_p) was measured by dynamic light scattering (Otsuka Photol LPA 3000/3100). The reported d_p data represent the average of at least seven measurements. The zeta potential (ζ) of the latex particles was determined using a Malvern Zetamaster. The pH 7 tris(hydroxymethyl)amino-methane buffer (20 mM) was used as the dilution solution for the latex sample [latex/buffer = 1/5 (v/v)]. The reported ζ data represent the average of at least five measurements. The latex particles were precipitated by an excess of methanol, followed by thorough washes with methanol and water to remove residual SDS, C_5OH and other impurities. The monomer conversion (X) was then determined by the gravimetric method. The molecular weight and molecular-weight distribution of polystyrene were determined by gel permeation chromatography (Waters 515/2410/Styragel HR2, HR4 and HR6).

Results and discussion

Formation of O/W microemulsions

The pseudo three-component phase diagram for the SDS/ C_iOH ($i = 4-6$)-stabilized ST microemulsions is shown in Fig. 1. Note that the C_4OH -containing gel phase was not observed within the composition range studied. Furthermore, the range of the microemulsion region in decreasing order is $C_4OH > C_5OH > C_6OH$. The viscosity and conductivity data are shown as a

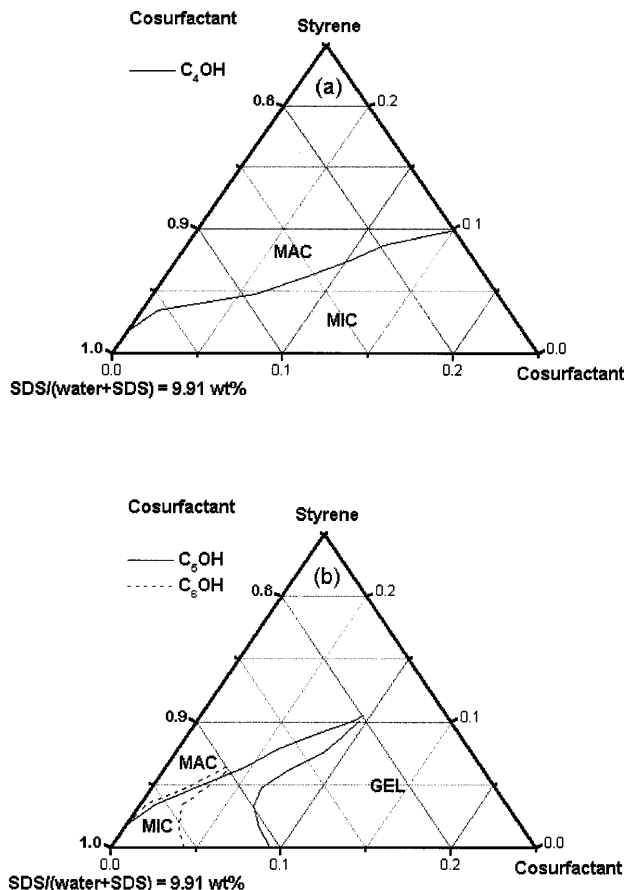


Fig. 1a, b Pseudo three-component phase diagram for the sodium dodecyl sulfate (SDS)/ C_iOH ($i = 4-6$)-stabilized styrene (ST) microemulsions. **a** 1-butanol (C_4OH), **b** (—) 1-pentanol (C_5OH), (---) 1-hexanol (C_6OH): MAC, MIC and GEL represent milky macroemulsion, transparent microemulsion and lamellar gel phase, respectively

function of the cosurfactant concentration in Figs. 2 and 3, respectively, for the recipe containing 25 g water, 381 mM SDS and 569 mM ST. For the C_5OH and C_6OH systems, the viscosity remains relatively constant when the macroemulsion is transformed into a microemulsion. This is followed by a rapid increase in viscosity when the transition from the microemulsion to the lamellar gel phase occurs (Fig. 2b, c). The conductivity first increases to a maximum when the macroemulsion is transformed into a microemulsion. The increased conductivity is attributed to the reduced oil droplet size (i.e., the enhanced mobility of droplets). The higher the mobility of the negatively charged droplets, the higher the conductivity of the macroemulsion or microemulsion [18]. Immediately after the formation of the lamellar gel phase, the conductivity starts to drop sharply (Fig. 3b, c). This is simply because the viscosity of lamellar gel phase builds up rapidly and the mobility of the ions within the structured gel phase

is greatly retarded as the cosurfactant concentration is further increased.

In contrast, the maximum viscosity is observed for the C_4OH system when the macroemulsion is transformed into a microemulsion (Fig. 2a). The initial increase in viscosity is probably due to the following two competitive factors. First, the fraction of the relatively hydrophilic C_4OH dissolved in the aqueous

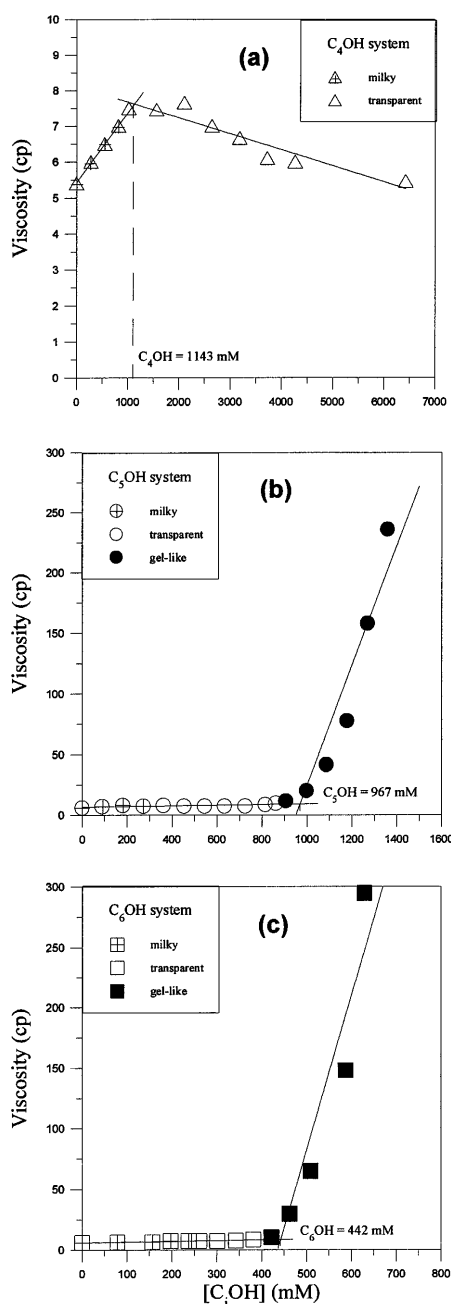


Fig. 2a–c Viscosity as a function of the cosurfactant concentration for the recipe containing 25 g water, 381 mM SDS and 569 mM ST. **a** C_4OH , **b** C_5OH , **c** C_6OH

phase cannot be ignored and, consequently, the volume fraction of the aqueous phase increases with increasing C_4OH concentration. This dilution effect may reduce the viscosity of the macroemulsion. On the other hand, the oil droplets become smaller (or the number of droplets increases) as more C_4OH molecules are incorporated into the droplet surface layer. The interactions among these droplets may thus be greatly enhanced, thereby leading to the increased resistance toward the applied shear force. It is then postulated that the latter effect overrides the former and, therefore, the viscosity increases with increasing C_4OH concentration (0 → 1100 mM). When the C_4OH concentration exceeds 1100 mM, the rate of change in the microemulsion droplet size with C_4OH concentration diminishes. Under these circumstances, the dilution effect provided by C_4OH dissolved in water comes into play and the viscosity starts to decrease with increasing C_4OH concentration. As for the C_5OH and C_6OH systems, the conductivity of the macroemulsion increases with increasing C_4OH concentration. It is, however, interesting to note that the conductivity of the microemulsion decreases with increasing C_4OH concentration (Fig. 3a). This trend is caused by the previously mentioned dilution effect in combination with the decreased dielectric constant of the aqueous solution. It is shown that both the viscosity and conductivity are sensitive to changes in the colloidal structure except for the transition from macroemulsion to microemulsion for the C_5OH and C_6OH samples monitored by viscosity measurement. The data of the molar ratio of cosurfactant to SDS at the point at which the transition from macroemulsion to microemulsion (or from microemulsion to lamellar gel phase) occurs, determined by the naked eye and measurements of viscosity and conductivity, are consistent with one another (Table 1).

The solubilities of C_4OH and C_5OH in water are 7.4 and 2.7 g per 100 g water, respectively, and C_6OH is

Table 1 Molar ratio of cosurfactant to sodium dodecyl sulfate (SDS) at the point at which the transition from macroemulsion (MAC) to microemulsion (MIC) or from MIC to lamellar gel phase (GEL) occurs (recipe = 25 g water + 381 mM SDS + 569 mM styrene, ST) for 1-butanol (C_4OH), 1-pentanol (C_5OH) and 1-hexanol (C_6OH)

	C_4OH	C_5OH	C_6OH
MAC → MIC	2.66 ^a 3.00 ^b 2.44 ^c	0.99 ^a 1.15 ^c	0.69 ^a 0.71 ^c
MIC → GEL	—	2.41 ^a 2.54 ^b 1.95 ^c	1.02 ^a 1.16 ^b 0.97 ^c

^a Determination from the phase diagram

^b Determined from viscosity

^c Determined from conductivity

slightly soluble in water (the Merck Index). The values of the hydrophile-lipophile balance (HLB) for C₄OH, C₅OH and C₆OH estimated by the group contribution method [19] are 7, 6.53 and 6.05, respectively. These HLB data are in the range between the O/W emulsifier (HLB = 8–18) and water-in-oil emulsifier (HLB = 3.5–6); therefore, these C_{*i*}OH (*i* = 4–6) molecules tend to adsorb onto the microemulsion droplet surface layer. It is most likely that the difference in the surface activity of C_{*i*}OH is responsible for the quite different cosurfactant performance between C₄OH and C₅OH (or C₆OH). Guo et al. [20] showed that the fraction of C₅OH partitioned among the various phases of the ST microemulsion in decreasing order is interface \gg oil phase $>$ aqueous phase. It was found that the molar ratio of C₅OH to SDS at the oil–water interface is around 0.9. In this work, the molar ratio of all the added C₅OH to SDS at the point at which the transition from macroemulsion to microemulsion occurs is about 1.1 (Table 1), which is consistent with the work of Guo et al. When the microemulsion starts to form, the molar ratio of all the added C₆OH to SDS is only 0.7. This result suggests that it is more efficient for C₆OH to adsorb onto the droplet surface layer than for C₅OH. Nevertheless, much less C₆OH is required for the colloidal system to reach the region of the lamellar gel phase (the molar ratio of all the added C_{*i*}OH to SDS is 1.1 for the C₆OH system and 2.3 for the C₅OH system, Table 1). Thus, the C₆OH-containing microemulsion region is the narrowest. In contrast, in addition to the oil–water interface, a significant fraction of C₄OH can partition in

the aqueous phase due to the relatively hydrophilic nature of C₄OH. As a result, a value of 2.7 for the molar ratio of all the added C₄OH to SDS is required for the transition from macroemulsion to microemulsion to occur (Table 1). Furthermore, no lamellar gel phase is observed within the composition range studied since more C₄OH molecules can be accommodated in the aqueous phase in comparison with the C₅OH system (Fig. 1). This result implies that C₄OH is less efficient in preparing microemulsions and the C₄OH-containing microemulsion region is the broadest.

Microemulsion polymerization

The recipe and some experimental results obtained from the ST microemulsion polymerizations with various levels of C_{*i*}OH (*i* = 4–6) are compiled in Tables 2–4 (see C41–C45 in Table 2, C51–C54 in Table 3 and C61–C64 in Table 4). The influence of the cosurfactant concentration on the size (d_p) and number (N_p) of microemulsion polymer particles is shown in Fig. 4. In this series, the microemulsion comprises 25 g water, 381 mM SDS, 0.1 mM NaHCO₃, 577 mM ST for the C₄OH and C₅OH systems (462 mM ST for the C₆OH system), 0.5 mM Na₂S₂O₈ and various levels of C_{*i*}OH. It is shown that d_p increases (or N_p decreases) with increasing C₄OH concentration, whereas d_p (or N_p) is relatively insensitive to changes in the C₅OH or C₆OH concentration. This is probably due to the increased C₄OH concentration in water. As a result, the dielectric

Table 2 Recipe and some experimental results obtained from the ST microemulsion polymerization with C₄OH as the cosurfactant

	C41	C42	C43	C44	C45	C46	C47	C48
[C ₄ OH](%)	5.49	6.40	7.87	9.30	8.00	7.92	7.85	7.80
[ST] (%)	4.85	4.80	4.72	4.65	3.20	4.12	5.02	5.62
<i>X</i> (%)	96.9	97.3	92.3	96.0	91.2	87.2	93.9	91.9
$M_w \times 10^{-6}$ (g/mol)	4.47	4.25	3.13	4.33	3.16	3.53	3.42	3.14
Polydispersity index	2.97	3.27	5.44	2.47	2.14	2.13	1.59	4.35
No. of polymer chains per particle	7.6	8.8	13.7	10.5	7.4	7.2	9.5	18.7
ζ (mV)	−23.8	−46.0	−22.3	−46.5				
Total scrap (%)	0.0097	0.012	0.012	0.047	0.018	0.017	0.023	0.015

Table 3 Recipe and some experimental results obtained from the ST microemulsion polymerization with C₅OH as the cosurfactant

	C51	C52	C53	C54	C55	C56	C57
[C ₅ OH](%)	3.31	3.94	4.88	5.80	4.96	4.83	4.80
[ST] (%)	4.96	4.93	4.88	4.83	3.31	5.80	6.40
<i>X</i> (%)	95.4	92.4	91.8	93.6	90.2	87.6	89.3
$M_w \times 10^{-6}$ (g/mol)	4.20	5.10	3.95	4.32	3.08	3.96	3.59
Polydispersity index	1.83	4.45	1.68	4.78	2.36	4.47	2.31
No. of polymer chains per particle	5.4	4.5	6.0	5.5	5.8	6.9	8.1
ζ (mV)	−7.9	−27.6	−13.3	−24.8			
Total scrap (%)	0.0074	0.0071	0.0062	0.010	0.011	0.0075	0.0067

Table 4 Recipe and some experimental results obtained from the ST microemulsion polymerization with C₆OH as the cosurfactant

	C61	C62	C63	C64	C65	C66	C67
[C ₆ OH](%)	1.36	1.70	2.03	2.36	2.38	2.35	2.33
[ST] (%)	4.09	4.07	4.06	4.05	3.40	4.37	5.32
<i>X</i> (%)	92.8	90.7	97.7	98.9	82.2	80.7	83.3
<i>M_w</i> × 10 ⁻⁶ (g/mol)	3.89	3.76	3.99	3.25	3.61	3.43	3.61
Polydispersity index	9.09	11.28	3.46	2.36	2.19	3.01	1.65
No. of polymer chains per particle	4.8	5.4	5.5	7.2	5.2	7.2	8.2
ζ (mV)	-6.3	-12.1	-7.4	-6.1			
Total scrap (%)	0.0067	0.0039	0.0062	0.0056	0.0078	0.0075	0.0068

constant of the aqueous phase (i.e., the electrostatic repulsion force between two approaching latex particles) is greatly reduced and flocculation among the relatively unstable particles may occur. The total scrap data also show that the C₄OH-stabilized particles are less stable in comparison with the C₅OH and C₆OH counterparts (see C41–C44, C51–C54 and C61–C64 in Tables 2–4). As a matter of fact, a significant amount of coagulum was observed 20–30 min after the start of polymerization for the system with a C₄OH concentration of 5397 mM. The initial microemulsion droplet size (*d_d*) was not measured and the literature value of *d_d* (4.12 nm) for the C₅OH-containing ST microemulsion is used in the following calculation since the recipe used in this work is quite similar to the one used by Guo et al. [20]. Thus, the initial number of droplets (*N_d*) in the C₅OH system is estimated to be 4.55×10^{19} . The ratio N_d/R_i represents the time required for all the droplets to capture one free radical from the aqueous phase, where $R_i = 2f/k_d[I]$ is the generation rate of free radicals in water ($4.09 \times 10^{14} \text{ s}^{-1}$), *f* is the initiation efficiency factor (1), *k_d* is the initiator decomposition rate constant ($2.72 \times 10^{-5} \text{ s}^{-1}$ [21]) and [*I*] is the initiator concentration (0.5 mM). The fact that N_d/R_i ($1.11 \times 10^5 \text{ s}$) is about one order of magnitude greater than the reaction time ($2.88 \times 10^4 \text{ s}$) and that the average *d_p* for the C₅OH system (about 41 nm, Fig. 4a) is much larger than *d_d* (4.12 nm) suggests that only a small fraction of the initial droplets can be successfully nucleated. The remaining droplets serve as a reservoir to provide the growing latex particles with ST, SDS and C₅OH. Another possible explanation for the tenfold increase in *d_p* is the flocculation among the interactive latex particles due to the greatly reduced compatibility between the C₅OH and polystyrene produced. This factor will result in desorption of C₅OH out of the latex particle surface and, thereby, reduce the colloidal stability of the latex particles.

Polystyrene with very high molecular weight (10^6 g/mol) was produced in the microemulsion polymerizations with various levels of C_{*i*}OH (*i* = 4–6), as shown by the weight-average molecular weight (*M_w*) and polydispersity index ($\text{PDI} = M_w/M_n$, where *M_n* is the

number-average molecular weight of polystyrene) data in Tables 2–4. Figure 5 shows that both *M_w* and *M_n* decrease with increasing C₄OH and C₅OH concentration. As to the C₆OH system, *M_w* decreases but *M_n* increases with increasing C₆OH concentration. The reason for this is not clear at this point in time. The reciprocal of the number-average degree of polymerization ($1/X_n$) equals the chain transfer to monomer constant ($C_m = 4.5 \times 10^{-5}$ at 60 °C [22]) provided that each latex particle contains only one free radical until chain transfer to monomer occurs. Note that the value of *C_m* at 70 °C is expected to be larger than that at 60 °C and, thus, the estimated values of *X_n* (2.22×10^4) and *M_n* ($2.31 \times 10^6 \text{ g/mol}$) represent the upper limits of *X_n* and *M_n*, respectively, for the C₅OH system. The upper limit of *M_n* is greater than or equal to the experimental data ($0.90\text{--}2.35 \times 10^6 \text{ g/mol}$) obtained from the polymerizations with various levels of C₅OH. This result suggests that chain transfer to C_{*i*}OH and/or bimolecular termination of free radicals belonging to two latex particles upon collision may take place. The bimolecular termination may involve

1. Two long-chain radicals (*M_n* greater than the upper limit).
2. One long-chain radical and one short-chain radical (*M_n* equal to or smaller than the upper limit).
3. Two short-chain radicals (*M_n* much smaller than the upper limit).

This scenario results in a value of *M_n* equal to or smaller than the upper limit. The $1/X_n$ versus [C_{*i*}OH]/[ST] data, in which [ST] represents the initial ST concentration based on total water are shown in Fig. 6. Note that all the *M_n* ($X_n = M_n/104$) data obtained from this work are included in this plot. Although the data are quite scattered, the slope of the least-squares best-fitted straight line for the $1/X_n$ versus [C_{*i*}OH]/[ST] data is the average chain transfer to C_{*i*}OH (*i* = 4–6) constant (8.88×10^{-6}). The scattered molecular-weight data (see the *M_w* and PDI data in Tables 2–4 and the *M_n* data in Fig. 6) are attributed to the complicated polymerization mechanisms (e.g., flocculation among the interactive latex particles). With the *d_p* and *M_w* data, the number of

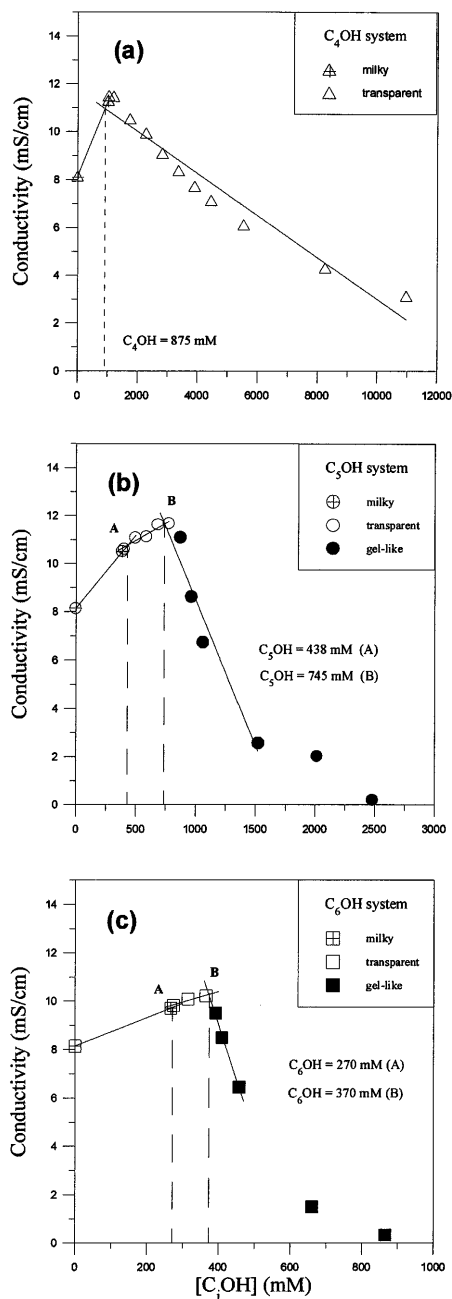


Fig. 3a–c Conductivity as a function of the cosurfactant concentration for the recipe containing 25 g water, 381 mM SDS and 569 mM ST. **a** C_4OH , **b** C_5OH , **c** C_6OH

polystyrene chains per latex particle can be estimated (Tables 2–4). The average numbers of polystyrene chains per particle are about 10, 5 and 6 for the C_4OH , C_5OH and C_6OH systems, respectively. This result also supports the postulation that the degree of flocculation of the latex particles in decreasing order is $C_4OH > C_5OH \sim C_6OH$ since the probability for latex particles to capture more than one free radical is rather low.

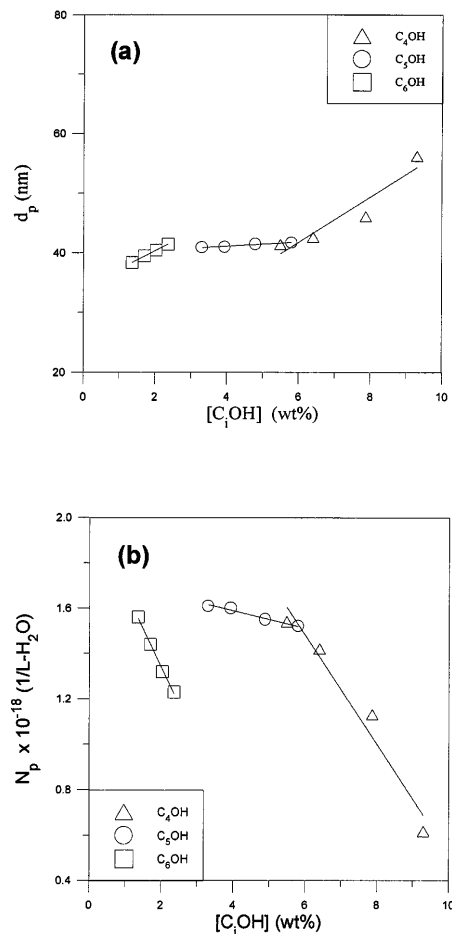


Fig. 4a, b Effect of the cosurfactant concentration on **a** the size and **b** the number of microemulsion polymer particles: the recipe contains 25 g water, 381 mM SDS, 0.1 mM $NaHCO_3$, 577 mM ST for C_4OH (577 mM ST for C_5OH , 462 mM ST for C_6OH) and 0.5 mM $Na_2S_2O_8$. C_4OH (\triangle), C_5OH (\circ), C_6OH (\square)

There is no apparent correlation between ζ of the latex particles and the C_iOH ($i = 4-6$) concentration (Tables 2–4). However, d_p seems to show a significant influence on ζ . The average d_p and $|\zeta|$ for the C_iOH ($i = 4-6$) system in decreasing order are 49.4 nm and 34.7 mV (C_4OH) > 41.3 nm and 18.4 mV (C_5OH) > 39.9 nm and 8.0 mV (C_6OH), i.e., the larger the value of d_p , the greater the absolute value of ζ . This is because the SDS concentration was kept constant at 381 mM throughout this series of experiments and more SDS molecules were available for stabilizing the larger latex particles (i.e., smaller oil–water interfacial area). As previously discussed, the SDS/ C_4OH -stabilized microemulsion polymerization is the least stable and limited flocculation of latex particles may occur. As a result, larger latex particles with a higher particle surface charge density are produced in order to survive the hostile aqueous environment.

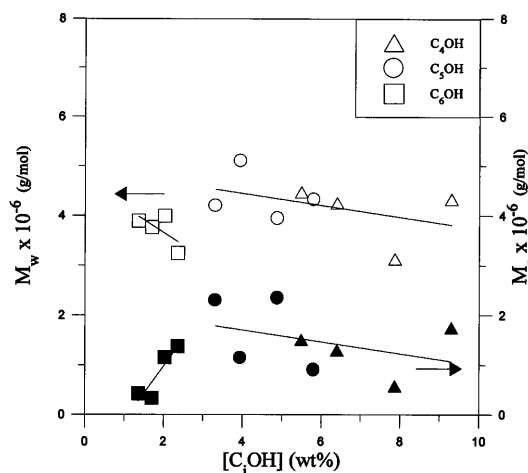


Fig. 5 Weight-average and number-average molecular weights of polystyrene as a function of the cosurfactant concentration. C_4OH (Δ), C_5OH (\circ), C_6OH (\square) (open and closed symbols represent weight-average and number-average molecular weights, respectively)

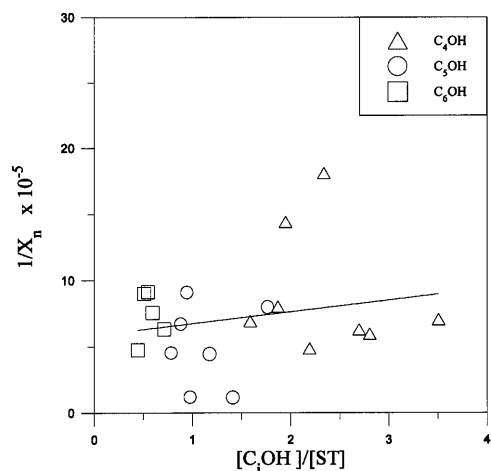


Fig. 6 Reciprocal of the number-average degree of polymerization as a function of the molar ratio of C_iOH ($i = 4-6$) to ST. C_4OH (Δ), C_5OH (\circ), C_6OH (\square)

The recipe and some experimental results obtained from the ST microemulsion polymerizations with various levels of ST are compiled in Tables 2–4 (see C43, C45–C48 in Table 2, C53, C55–C57 in Table 3 and C64–C67 in Table 4). The effect of the ST concentration on d_p and N_p is shown in Fig. 7. In this series, the microemulsion comprises 25 g water, 381 mM SDS, 0.1 mM $NaHCO_3$, 1349 mM C_4OH (or 681 mM C_5OH or 274 mM C_6OH), 0.5 mM $Na_2S_2O_8$ and various levels of ST. It is shown that both d_p and N_p increase simultaneously with increasing ST concentration, simply because more and larger microemulsion droplets form in the aqueous solution. It is also interesting to note that both the d_p and N_p data as a function of ST concen-

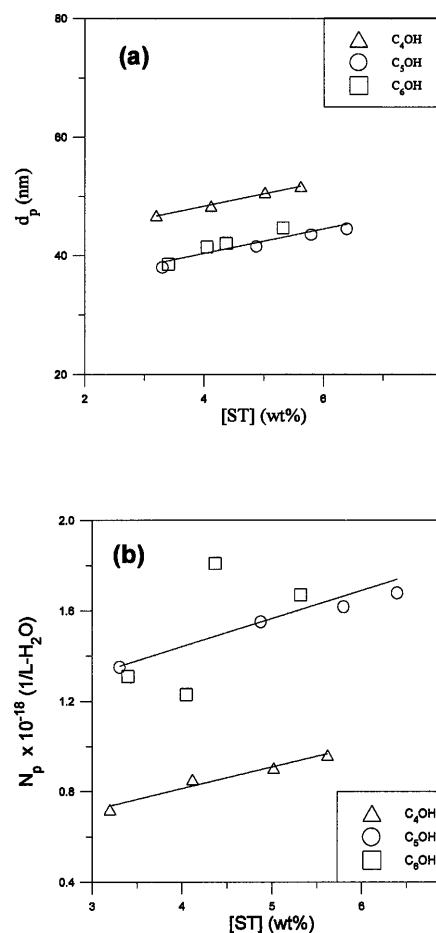


Fig. 7a, b Effect of the ST concentration on **a** the size and **b** the number of microemulsion polymer particles: the recipe contains 25 g water, 381 mM SDS, 0.1 mM $NaHCO_3$, 1349 mM C_4OH (or 681 mM C_5OH or 274 mM C_6OH) and 0.5 mM $Na_2S_2O_8$. C_4OH (Δ), C_5OH (\circ), C_6OH (\square)

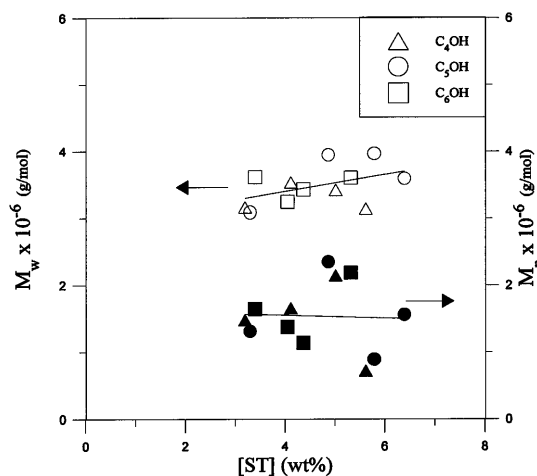


Fig. 8 Weight-average and number-average molecular weights of polystyrene as a function of the ST concentration. C_4OH (Δ), C_5OH (\circ), C_6OH (\square) (open and closed symbols represent weight-average and number-average molecular weights, respectively)

tration can be reasonably described by a single straight line for the C₅OH and C₆OH systems. On the other hand, the d_p or N_p data obtained from the C₄OH system fall on a straight line which is far from the least-squares best-fitted line for the C₅OH and C₆OH systems. M_w and M_n are shown as a function of ST concentration in Fig. 8. Although the data are rather scattered, the molecular weight of polystyrene seems to increase slightly with increasing ST concentration. As expected, more monomer molecules are available for the propa-

gation reaction of polymeric radicals when the ST concentration increases. The number of polystyrene chains per particle increases with increasing ST concentration (C43, C45–C48 in Table 2, C53, C55–C57 in Table 3 and C64–C67 in Table 4). Furthermore, the average number of polystyrene chains per particle for the C_iOH ($i = 4-6$) system in decreasing order is 11.3 (C₄OH) > 6.9 (C₆OH) ~ 6.7 (C₅OH). This trend again infers that the C₄OH-containing microemulsion polymerization is relatively unstable.

References

1. Prince LM (1977) In: Prince LM (ed) *Microemulsions: theory and practice*. Academic, New York, pp 1–20, 91–131
2. Schulman JH, Riley DP (1948) *J Colloid Sci* 3:383
3. Hoar TP, Schulman JH (1943) *Nature* 152:102
4. Schulman JH, Friend JA (1949) *J Colloid Sci* 4:497
5. El-Aasser MS, Lack CD, Choi YT, Min TI, Vanderhoff JW, Fowkes FM (1984) *Colloids Surf* 12:79
6. Atik SS, Thomas JK (1981) *J Am Chem Soc* 103:4279
7. Johnson PL, Gulari E (1984) *J Polym Sci Polym Chem Ed* 22:3967
8. Jayakrishnan A, Shah DO (1984) *J Polym Sci Polym Lett Ed* 22:31
9. Kuo PL, Turro NJ, Tseng CM, El-Aasser MS, Vanderhoff JW (1987) *Macromolecules* 20:1216
10. Guo JS, El-Aasser MS, Vanderhoff JW (1989) *J Polym Sci Polym Chem Ed* 27:691
11. Perez-Luna VH, Puig JE, Castano VM, Rodriguez BE, Murthy AK, Kaler EW (1990) *Langmuir* 6:1040
12. Gan LM, Chew CH, Lye I, Imae T (1991) *Polym Bull* 25:193
13. Napper DH, Kim DR (1996) *Macromol Rapid Commun* 17:845
14. Falco JW, Walker RD, Shah DO (1974) *AIChE J* 20:510
15. Shah DO, Hamlin RM (1971) *Science* 171:483
16. Shah DO, Tamjeedi A, Falco JW, Walker RD (1972) *AIChE J* 18:1116
17. Lagues M, Sauterey C (1980) *J Phys Chem* 84:3503
18. Bard AJ, Faulkner LR (1980) *Electrochemical methods: fundamentals and applications*. Wiley, New York
19. Davies JT, Rideal EK (1963) *Interfacial phenomena*. Academic, New York
20. Guo JS, El-Aasser MS, Sudol ED, Yue HJ, Vanderhoff JW (1990) *J Colloid Interface Sci* 140:175
21. Kolthoff IM, Miller IK (1951) *J Am Chem Soc* 73:3055
22. Braks JG, Huang RYM (1978) *J Appl Polym Sci* 22:3111